Decorrelated movements of Shockley partial dislocations in the γ phase channels of nickel-based superalloys at intermediate temperature

Sonia Raujol, Mustafa Benyoucef, Didier Locq, Pierre Caron, Florence Pettinari-Sturmel, Nicole Clément, Armand Coujou

Decorrelated movements of Shockley partial dislocations in the γ phase channels of nickel-based superalloys at intermediate temperature

Journal:	*Philosophical Magazine & Philosophical Magazine Letters*
Manuscript ID:	TPHM-05-May-0265
Journal Selection:	Philosophical Magazine
Date Submitted by the Author:	18-May-2005
Complete List of Authors:	Raujol, Sonia; CEMES Benyoucef, Mustafa; Faculte des sciences et Techniques Guéliz, Marrakech Locq, Didier; ONERA, DMMP CARON, Pierre; ONERA, DMMP Pettinari-Sturmel, Florence; CEMES / CNRS Clément, Nicole; CEMES COUJOU, Armand; CEMES
Keywords:	Ni-based superalloys, creep, in-situ electron microscopy
Keywords (user supplied):	stacking fault energy

Decorrelated movements of Shockley partial dislocations in the γ phase channels of nickel-based superalloys at intermediate temperature

S. RAUJOL*, M. BENYOUCEF**,
D. LOCQ***, P. CARON***,
F. PETTINARI*, N. CLEMENT* and A. COUJOU*

* CEMES/CNRS, 29 rue J. Marvig, 31055 Toulouse Cedex (France)
** FACULTE DES SCIENCES ET TECHNIQUES Guéliz, Marrakech (Maroc)
*** ONERA, 29 Avenue de la Division Leclerc, B.P.72, F-92322 Châtillon (France)

ABSTRACT

In nickel-based superalloys with high volume fraction of γ' precipitates, dislocations have to experience high curvatures in order to enter narrow channels by glide in the {111} planes of the f.c.c. γ matrix. Observation of *in situ* dynamic sequences performed in a Transmission Electron Microscope on several industrial superalloys have shown the occurrence of decorrelated movements of Shockley partial dislocations, originating from perfect dislocation dissociation. By evaluating the effective stress acting on each one of these partial dislocations, as well as their respective flexibility, the possible occurrence of such movements for some particular dislocation characters and channel widths is accounted for. These movements can play an important role in the creep behaviour of these materials in the low deformation rate regime.

Keywords: superalloy, creep, *in situ* experiment, high temperature, stacking fault energy.

§1. INTRODUCTION

For several years, the basic plastic deformation mechanisms operating at elevated temperature in nickel-based superalloys strengthened by γ'-Ni_3Al type precipitates were studied through the use of *in situ* straining experiments in a Transmission Electron Microscope (TEM). With this technique, the only one which allows direct observation of the evolution of the dislocation microstructure under stress and temperature, we have already identified such mechanisms in single-phased γ'-based monocrystals (Clément, Molénat and Caillard 1991, Lours, Coujou and Coulomb 1991, Benyoucef, Clément and Coujou 1995) as well as in single-phased γ

monocrystals simulating the matrix of various industrial single crystal superalloys (Jouiad, Pettinari, Clément and Coujou 1999).

The core structure of the a/2<110> dislocations propagating in the γ matrix of superalloys has been described by a number of authors (Kear, Giamei, Silcock and Ham 1968, Kear, Giamei, Leverant, and Oblak 1969, Guimier 1972, Condat and Décamps 1987, Caron, Khan and Veyssière 1988). Saint-Antonin (1991) has shown that in a polycrystalline γ/γ' superalloy (Astroloy) containing a volume fraction of about 45% of precipitates with sizes within the range 20 nm-100 nm, the dissociation of single matrix dislocations which occurs in the γ phase at 650°C can lead to the decorrelated movement of two a/6<112> Shockley partial dislocations. The mechanism operates under specific stress conditions: relaxation following loading, at a low strain rate (~ 10^{-6} s^{-1}) and small total strain (less than one percent).

The aim of this work is to demonstrate, through the analysis of *in situ* deformation images, the conditions for these decorrelation processes to occur. The study was carried out on two different industrial superalloys with a γ' volume fraction in the range 50 and 70 percent. This micro-mechanism is analysed in detail from *post mortem* observations. The effective force acting on each partial of the moving dislocations is evaluated taking into account the difference in flexibility of a perfect dislocation compared to a partial one.

§2. MATERIALS AND EXPERIMENTAL TECHNIQUE

The chemical compositions of the MC2 and NR3 superalloys are given in Table 1. The MC2 nickel-based superalloy is used for single crystal turbine blade applications in gas turbine engines. <001>-oriented single crystal bars were directionally solidified at ONERA by using the withdrawal process. After standard homogenization and ageing heat treatments, it contains a homogeneous monomodal distribution of almost cubical γ' precipitates with a volume fraction close to 70%. *In situ* tensile experiments were conducted at 850°C along a <001> orientation that corresponds to the direction of the centrifugal stress acting on the blade.

The powder metallurgy NR3 superalloy was designed for compressor and turbine disk applications. The material used in this study was produced by TECPHY and SNECMA using the following industrial route: vacuum induction melted ingot, argon atomisation, powder

sieving (-200 mesh), hot extrusion, isothermal forging. A γ' supersolvus heat treatment followed by standard ageing heat treatments produce a mean grain size of about 50 μm and a bimodal distribution of γ' precipitates within the grains (γ' volume fraction around 50%). *In situ* tensile experiments were conducted at 25°C on NR3 specimens previously creep-strained at 700°C.

The experimental details of the TEM *in situ* straining technique used here have already been reported (Couret, Crestou, Farenc, Molénat, Clément, Coujou and Caillard 1993). Due to the high stress level needed for activation of the deformation in γ'-strengthened superalloys (highly resistant material and elevated temperature), curved specimens (Coujou, Lours, Roy, Caillard and Clément 1990) were used so as to concentrate the stress in the area under observation.

§3. EXPERIMENTAL RESULTS

The typical γ/γ' microstructures existing in the NR3 and MC2 alloys are shown in figure 1. In the polycrystalline NR3 superalloy, the bimodal distribution of γ' precipitates is clearly illustrated in figure 1a. The distance between the small γ' particles is variable and there is a denuded zone between the small tertiary γ' precipitates and the large secondary ones. In the single crystal MC2 superalloy (figure 1b), the distribution of γ' precipitates is monomodal and appears to be much more regular than in NR3. Mean values of the size of the γ' precipitates and of the width of the γ channels are reported in Table 2 for the both alloys. They have been calculated from more than 100 measurements.

A typical *post mortem* dislocation configuration observed in NR3 after creep at 700°C and 650 MPa (0.2 % of deformation) is shown in figure 2a. A perfect dislocation, whose Burgers vector DA (Thompson notation) is deduced from several images taken with different diffraction conditions, is noted ijkl. It is pushed close to P_1 and P_2 precipitates. In the matrix channel existing between them, this dislocation has broken up in two partial dislocations noted 1 and 2, whose Burgers vectors are respectively Dβ and βA. While moving within the channel, partial 1 has left a stacking fault while, behind, partial 2 remained curved at the channel entrance. A similar process can be observed on the other side of the same channel, where a dislocation

noted mnop appears also dissociated into two partial dislocations. Other examples, in another area of the same alloy, are presented in figure 2b and indicated by arrows. In this figure, it must be noted that this decorrelation process is not observed everywhere. As it will be discussed later, it depends on the width of the channel and on the character of the entering dislocation.

A dynamic sequence recorded, for the same alloy, during a straining experiment at 20°C, is shown figure 3. At the beginning (figure 3a), in the channel underlined by dots, dislocation i is already spread in two partials 1 and 2. On the following images (figures 3b and 3c), partial 1 continues to propagate, while partial 2 remains quite immobile.

A similar sequence, now in the MC2 superalloy, is presented figure 4 during a straining experiment at 850°C. In picture 4a, the single dislocation P, which is gliding into the (111) plane, is already dissociated into two Shockley partial dislocations denoted i and j. This dissociation, which takes place in a channel perpendicular to the tensile axis X, is extending in pictures b and c until the leading Shockley dislocation i crosses the whole channel. The measured dislocation rate is very low: v = 3.5 nm/s. On the other hand, the trailing partial dislocation j remains arrested at the entrance of this channel.

Now, a shearing event of γ' precipitates, initiated by such a decorrelation process, is visible in NR3 crept at 700°C under 650 MPa (0.2 % of deformation) (figure 5). The leading partial p_1 propagates from the left to the right and shears the γ' precipitates by an original way derived from the Condat-Décamps mechanism (Condat and Décamps 1987) and analysed in detail elsewhere (Décamps, Raujol, Coujou, Pettinari-Sturmel, Clément, Locq and Caron 2004). Here, a stacking fault is created in both γ and γ' phases and the trailing partial noted p_2 remains blocked. In the image, the sheared secondary and tertiary precipitates are merged within the stacking fault expanding in the whole $(\bar{1}11)$ plane.

§4. DISCUSSION

The two types of observations, carried out either *post mortem* or *in situ* on NR3 and MC2 respectively, share a common point: they correspond to decreasing transient stress states associated with relaxation. These dislocation configurations have seldom been investigated in depth in the past. Moreover, to our knowledge, these movements have never been reported in

superalloys with a high volume fraction of γ' phase. As a result, no explanation can be found until now for this mechanism, in the literature.

Here, an analysis will therefore be put forward based on the following idea: for a dislocation to propagate in a matrix channel, the effective resulting force on the dislocation segment must be in excess of the threshold force characterizing the local geometry of the obstacle and generally called the "Orowan stress" in previous models. Decorrelation of the partial dislocations movement occurs when the effective force acting on the perfect dislocation does not allow it to propagate as a whole, in the matrix channel, while this propagation is allowed for the leading partial dislocation alone.

To quantify this, it is necessary to evaluate the effective force acting on the perfect dislocation and on each one of the partial dislocations. Then, for each dislocation, the threshold force taking into account the flexibility of each one of these dislocations will be calculated.

4.1. *Effective forces*

The effective force existing in the γ phase on each perfect dislocation segment or partial dislocation is the result of several contributions. Let us call $b\tau_{res}$ the resulting force where τ_{res} is obtained from the summation of the following components, resolved on the active glide plane of the dislocation:

- the applied shear stress τ_A,
- the local value of the internal shear stress τ_i which can either assist (+) or oppose (-) the applied stress,
- the local value of the friction stress τ_F which is always impeding the dislocation glide movement,
- the local value of the misfit stress τ_M which can either assist (+) or oppose (-) the dislocation glide. This shear stress can be deduced from the misfit stress tensor Σ_M through the expression:

$$\tau_M = (\Sigma_M.\mathbf{n}).\mathbf{b}/b \qquad (1)$$

where **n** is the glide plane normal and **b** is the Burgers vector .

(il faudrait définir le misfit. Que sont **b** et b, ainsi que n ?)

Of course, the situation is different for each partial. We shall write the forces acting on partial dislocation segments 1 and 2, which correspond respectively to the leading and the trailing partial dislocations:

$$F_{ef/1} = b_1\tau_{ef/1} = b_1\tau_{res/1} - \Gamma = b_1(\tau_{A/1} \pm \tau_{i/1} - \tau_{F/1} \pm \tau_{M/1}) - \Gamma \quad (2)$$

$$F_{ef/2} = b_2\tau_{ef/2} = b_2\tau_{res/2} + \Gamma = b_2(\tau_{A/2} \pm \tau_{i/2} - \tau_{F/2} \pm \tau_{M/2}) + \Gamma \quad (3)$$

where Γ is the stacking fault energy of the γ matrix.

The corresponding exerted force per unit length of dislocation pulls the leading dislocation backward and inversely attracts the trailing dislocation forward.

4.2. *Flexibility of dislocation - Orowan stress*

In the literature, the propagation stress necessary to move a dislocation on its glide plane, in a γ channel, is often referred to as the Orowan stress τ_{OR}. It is closely related to the dislocation flexibility that can be defined as the inverse of the line tension:

$$\zeta = f(b,\phi,T) \quad (4)$$

It is an intrinsic property of a dislocation segment, which depends on the nature of the dislocation through its Burgers vector b, on its character ϕ and on the temperature T through the elastic constants. A high flexibility will be characterized by a superior ability of the moving segment to propagate between obstacles by bowing out, to infiltrate γ matrix channels between γ' precipitates and thus percolate more easily through the γ - γ' maze.

The Orowan stress, for a given dislocation, is the threshold value which must be reached by the effective stress, in order for the bowing out segment, to move past two obstacles, separated by a distance d' in the {111} glide plane. For instance:

$$\tau_{OR}(b,\phi,d',T) = 2\zeta/bd' \quad (5)$$

So, this threshold stress depends on the intrinsic properties of the dislocation segment concerned, through ζ, as well as on extrinsic properties, through the local configuration of the obstacles and their distribution in space.

These line tension stresses have been determined using the De Witt and Koehler's relation (1959) which is a function of the energy of dislocation. This energy of the dislocation line W/l has been computed within the framework of anisotropic elasticity through use of the DISDI software (Douin 1987).

The curves of figure 6 show the variations of the line tension stress ζ as a function of the character ϕ of the dislocation respectively for *1)* a perfect undissociated dislocation, *2)* a partial belonging to a perfect dissociated dislocation and *3)* an isolated partial dislocation. In case *2)*, it is found that $\zeta_{screw} / \zeta_{edge} \approx 4.3$. The partial dislocation is much more flexible than the perfect dissociated one ($\zeta_{perf} / \zeta_{part} \approx 4$ for the screw portion). It can be also remarked that in the anisotropic calculation, the most rigid partial dislocation has a $\phi \approx 20°$ character.

4.3. *Conditions for the decorrelated movement of partial dislocations*

Let us now consider separately the possible behaviour of two Shockley partial dislocations 1 and 2 resulting from the dissociation of a perfect dissociated dislocation P, as they are confronted with an obstacle configuration (entrance of a γ channel, propagation inside a channel, by-passing a residual γ' island in the glide plane, etc). They are characterized by the Orowan threshold forces $F_{OR/P}$, $F_{OR/1}$ and $F_{OR/2}$. The existence of the decorrelation process depends on the width of the channel and occurs when the perfect dislocation P cannot enter, as a whole, the channel, which means that, in this case:

$$F_{ef/P} < F_{OR/P} \qquad (6)$$

Several cases must be examined:

A) $F_{ef/1} > F_{OR/1}$	**a)** $F_{ef/2} > F_{OR/2}$	Both partial dislocations overcome the obstacle and their movements remain correlated.
	b) $F_{ef/2} < F_{OR/2}$	Partial 1 alone overcomes the obstacle; partial 2 is stopped inducing the decorrelation.
B) $F_{ef/1} < F_{OR/1}$	**a)** $F_{ef/2} < F_{OR/2}$	Both partials are stopped.
	b) $F_{ef/2} > F_{OR/2}$	Both partials may overcome the obstacle if $F_{ef/2}$ is high enough to push partial 1 through the channel.

Cases Aa and Bb are fairly similar. In case Aa, both partials can overcome the Orowan threshold, whereas in case Bb, the leading partial cannot do it by itself and needs the help of the trailing partial. Case Ab describes the typical configuration capable of triggering decorrelation. These decorrelated movements occur when the stress on the leading partial dislocation and its flexibility are such that they compensate for its handicap which lies in pulling the stacking fault. Thus, they allow the movement to take place in the case where the perfect dislocation, which is too rigid or not sufficiently stressed, cannot cross the channel entrance.

Relations 2 and 3 give the physical parameters influencing the decorrelation process. The order of magnitude of the different terms is evaluated in the appendix in the particular case of the dislocation imaged figure 4. Applying equation (1), the effective stress on both the leading and the trailing partials can be estimated through the use of equations (2) and (3). In these expressions, the terms τ_A and τ_M can be computed with a fairly good level of accuracy. On the other hand, it is necessary to make assumptions on τ_F and Γ. Since the effect of the stacking fault energy is of opposite sign for each partial [equations (2) and (3)], the difference in resulting forces necessary to keep them apart and enforce their decorrelated movement is equal then to $2\,\Gamma$. Using the value of Γ measured close to 25 mJ/m^2 at room temperature by Benyoucef, Décamps, Coujou and Clément (1995), the decorrelation is unlikely. As

decorrelation is observed, the stacking fault energy is necessarily lower than above. This can be attributed to the presence of Suzuki effect (Suzuki 1952) possible in such an alloy containing several solute elements. This mechanism does not contribute much to the tensile strain at an imposed strain rate, but it can play an important role in relaxation or creep tests. In these cases, the levels of imposed stress are much less. Thus, the channel entrances play the role of effective dislocation filters favouring the movements of flexible partial dislocations rather than rigid perfect ones. They are able to select Shockley partial dislocations involved in the shearing of precipitates. In some cases, two Shockley dislocations are involved for the shearing (Kear et al. 1968 and 1969, Condat and Décamps 1987). But, the shearing process can be only due to the movement of the leading Shockley as shown in figure 5 for NR3. This new shearing process (Décamps et al 2004) is due to the decorrelation process. The partial p_1 alone, by propagating in channel from the left to the right, is at the origin of the stacking fault observed both in the matrix and the γ' precipitates. Such a micro-mechanism often visible as shown in figure 7, is considered as the signature of narrow corridors. This is in close correlation with the better creep properties observed in this material after suitable heat treatment (Locq et al. 2004) (the strain rate at 700°C and 650 MPa is $\dot{\varepsilon} \approx 3.6\ 10^{-9}\ s^{-1}$ when $\langle d \rangle \approx 52$ nm while $\dot{\varepsilon} \approx 1.5\ 10^{-9}\ s^{-1}$ when $\langle d \rangle \approx 33$ nm).

More generally, a large panel of mechanisms are possible. When the stress is sufficient, all of them can be used by the moving dislocations and the strain rate is controlled by the one producing the most effective strain. At lower stress levels, dislocations have to resort to more subtle movements compatible with the local geometry of obstacle they are facing.

§5. CONCLUSION

Decorrelated movements of partials belonging to the same perfect dislocation have been video recorded during *in situ* straining experiment, at 25°C and at 850°C, in γ matrix channels of NR3 and MC2 superalloys respectively. By calculating the different components of the stress acting on each partial, it is shown that the resulting effective stress acting on each of them can be very different conducing to the propagation of the leading one while the trailing is stopped at the entrance of a narrow channel.

These movements probably play a minor role in the tensile deformation of superalloys at room temperature, but are shown to clearly decrease their deformation rate during high temperature creep experiments even when the volume fraction of γ' phase is less important.

Acknowledgments:

The authors thank Professor J.L. Strudel for allowing them a true maturation of their ideas before writing and for his clear help in improving the manuscript. They are indebted to P. Veyssière for the concept of "channels filtering" the dislocations. They want to express their gratefulness to J. Crestou for his talent in the preparation of samples. A part of this study was financially supported by the RRIT "Recherche Aéronautique sur le Supersonique", Ministère de la Recherche et des Transports.

Appendix: Quantitative analysis of a specific case

As all the parameters involved in the afore mentioned analytical expressions (1), (2) and (3) are not known, reasonable assumptions have to be made in order to apply them to a specific case. Thus, it is assumed that:

• the perfect dislocation which glides into the plane $(\bar{1}\,\bar{1}\,1)$ of figure 4 has a Burgers vector DA (Thompson notation) and is split in this plane in Dγ (leading dislocation) and γA (trailing dislocation), Dγ is moving while γA is stopped. (NB : In the following, the perfect dislocation is noted by *p*, the first partial by *1* and the second one by *2*).

• the applied stress σ_A is taken equal to the resolved shear stress at 850 °C:

$$\sigma_A = 710 \text{ MPa}; \tau_{A/P} \approx 290 \text{ MPa}; \tau_{A/1} \approx 170 \text{ MPa and } \tau_{A/2} \approx 335 \text{ MPa},$$

• the crystalline misfit creates a bi-axial stress equal to 220 MPa (Müller, Glatzel and Feller-Kniepmeier 1992, Ganghoffer, Hazotte, Denis and Simon 1991) and the corresponding reduced stress on the dislocations is:

$$\tau_{M/P} \approx 100 \text{ MPa}; \tau_{M/1} \approx 50 \text{ MPa and } \tau_{M/2} \approx 104 \text{ MPa}.$$

These values are obtained by applying equation (1).

As the movement occurs without a pile-up multiplication effect, as the effective stress on this perfect dislocation $\tau_{ef/P} \approx 390$ MPa is less than $\tau_{OR} \approx 500$ MPa, it cannot propagate in this channel. In order to create a stress on the leading partial dislocation higher than $\tau_{OR/1} \approx 100$ MPa, it has to be assumed that $\Gamma \approx 10$ mJ/m^2 yielding for $\Gamma/b \approx 80$ MPa and $\tau_{ef/1} \approx 140 \text{ MPa} \geq \tau_{OR/1}$. This value of Γ is much less than the measured value at room temperature in this alloy (Benyoucef et al. 1995). In these conditions, the first partial can move and one gets $\tau_{ef/2} \approx 330$ MPa which is less than $\tau_{OR/2}$. Thus the propagation of the trailing partial is impeded.

REFERENCES

BENYOUCEF, M., CLEMENT, N., COUJOU, A., 1995, *Phil. Mag*. A, **72**, 1043-1056.

BENYOUCEF, M., DECAMPS, B., COUJOU, A., and CLEMENT, N., 1995, *Phil. Mag*., A, **71**, 4, 907-923.

CARON, P., KHAN, T., and VEYSSIERE, P., 1988, *Phil. Mag*. A, **6**, 859.

CLEMENT, N., MOLENAT, G., and CAILLARD, D., 1991, *Phil. Mag*., 697.

CONDAT, M., and DECAMPS, B., 1987, *Scripta Met*., **21**, 607.

COUJOU, A., LOURS, P., ROY, N.A., CAILLARD, D., and CLEMENT, N., 1990, *Acta Metall*, 825.

COURET, A., CRESTOU, J., FARENC, S., MOLENAT, G., CLEMENT, N., COUJOU, A., and CAILLARD, D., 1993, *Microsc. Microanal. Microstruct*., **4**, 1.

DE WITT, G., and KOEHLER, J. S., 1959, *Phys. Rev.*, 1113.

DECAMPS, B., RAUJOL, S., COUJOU, A., PETTINARI-STURMEL, F., CLEMENT, N., LOCQ, D., and CARON, P., 2004, *Phil Mag,* **84**, 91.

DOUIN, J., 1987, Thèse de l'Université de Poitiers, France.

GANGHOFFER, J.F., HAZOTTE, A., DENIS, S., and SIMON, A., 1991, *Scripta Metall*, **25**, 2491.

GUIMIER, A., 1972, Thèse de l'Ecole des Mines de Paris, France.

JOUIAD, M., PETTINARI, F**.,** CLEMENT, N., and COUJOU, A., 1999, *Phil. Mag.A,* **79**, 11, 2591.

KEAR, B.H., GIAMEI, A.F., SILCOCK, J.M., and HAM, R.K., 1968, *Scripta Metall*, **2**, 287.

KEAR, B.H., GIAMEI, A.F., LEVERANT, G.A., and OBLAK, J.M., 1969, *Scripta Metall*, **3**, 455.

LOCQ, D., CARON, P., RAUJOL, S., PETTINARI-STURMEL, F., COUJOU, A., CLEMENT, N., 2004, *Proceedings of Superalloys 2004*, edited by K. A. Green, H. Harada, T. E. Howson, T. M. Pollock, R. C. Reed, J. J. Schirra, S. Walston, TMS, Warrendale, Pa, U.S.A., 179-187.

LOURS, P., COUJOU, A., and COULOMB, P., 1991, *Acta Metall. Mater.*, **39,** 8, 1787.

MÜLLER, L., GLATZEL, U., and FELLER-KNIEPMEIER, M., 1992, *Acta metall*, 40, 6, 1321.

POLLOCK, T.M., ARGON, A.S., 1994, *Acta Metall. Mater.*, **42**, 1859.

SAINT-ANTONIN, F., 1991, Thèse de l'Ecole des Mines de Paris, France.

SUZUKI, H., 1952, *Sci. Rep. Res. Inst. Tohoku Univ.*, **A-4**, 452.

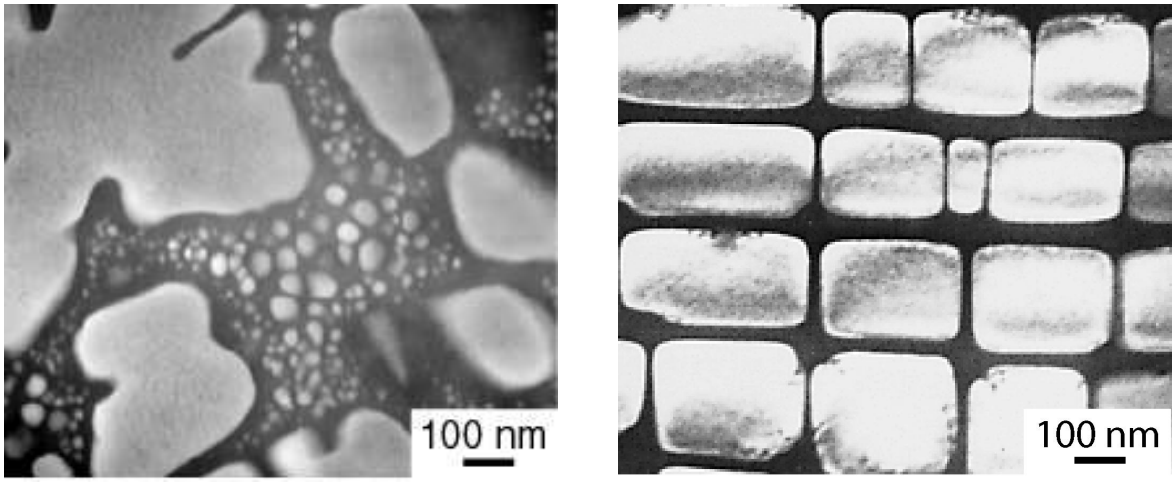

(a) (b)

Figure 1

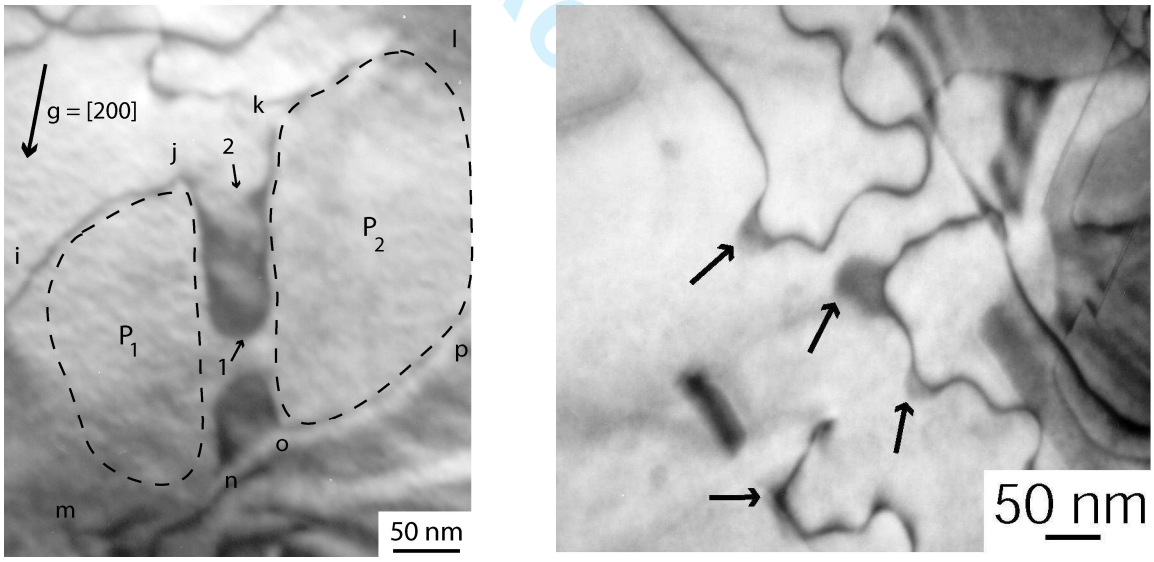

(a) (b)

Figure 2

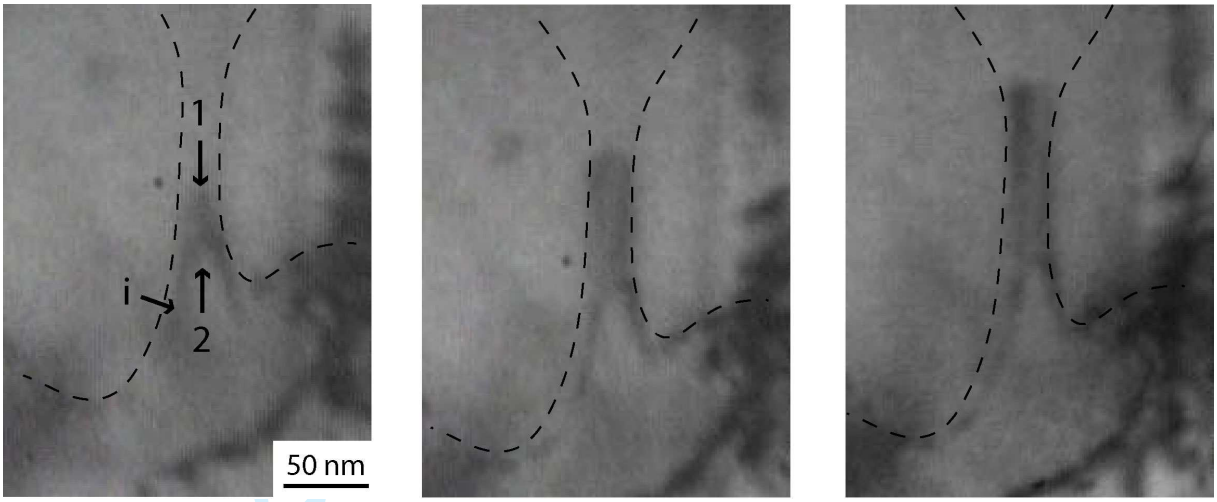

(a) (b) (c)

Figure 3

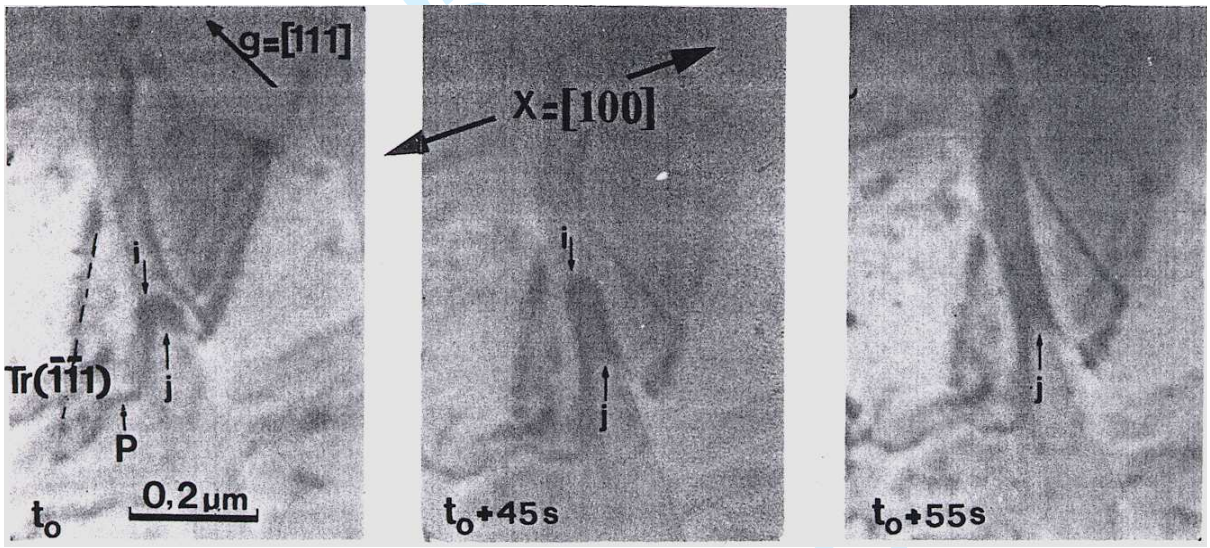

(a) (b) (c)

Figure 4

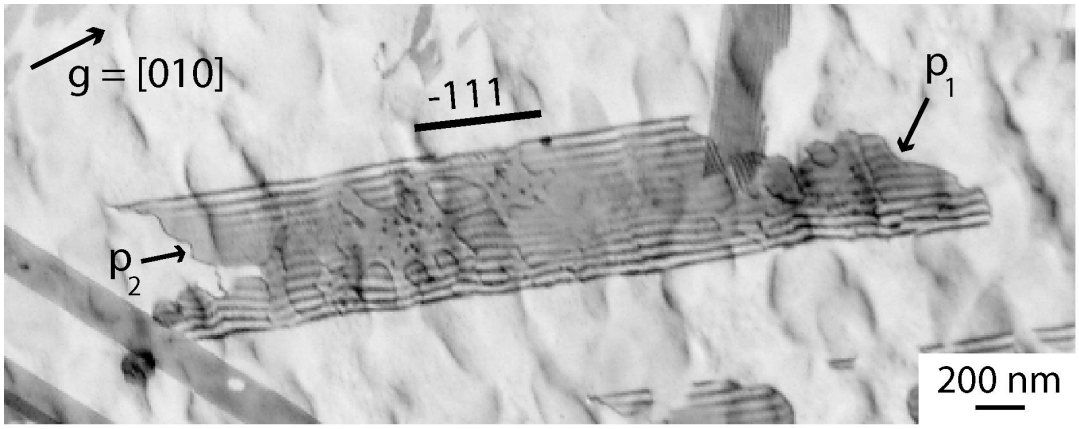

Figure 5

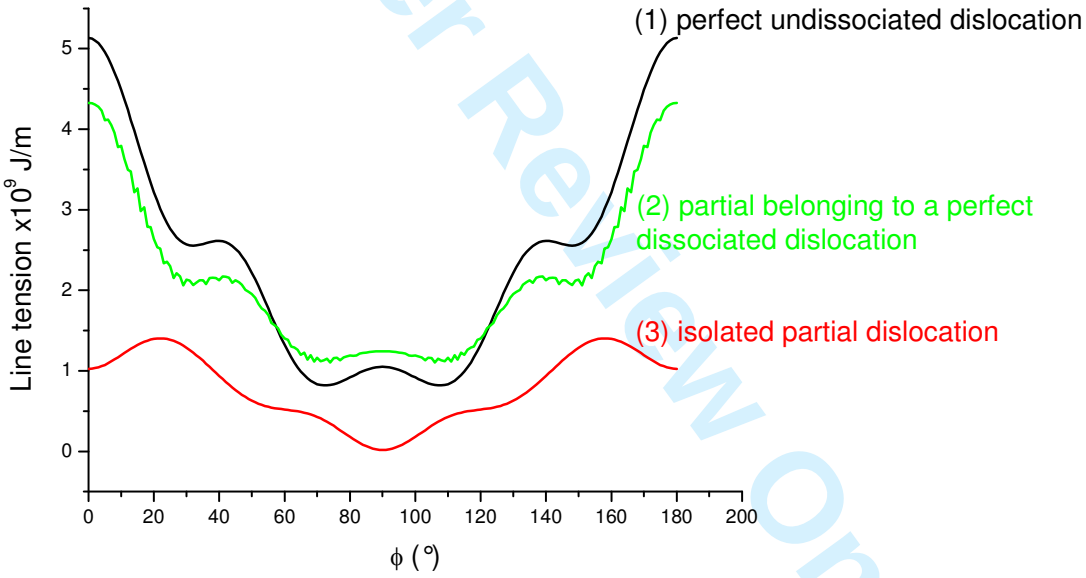

Figure 6

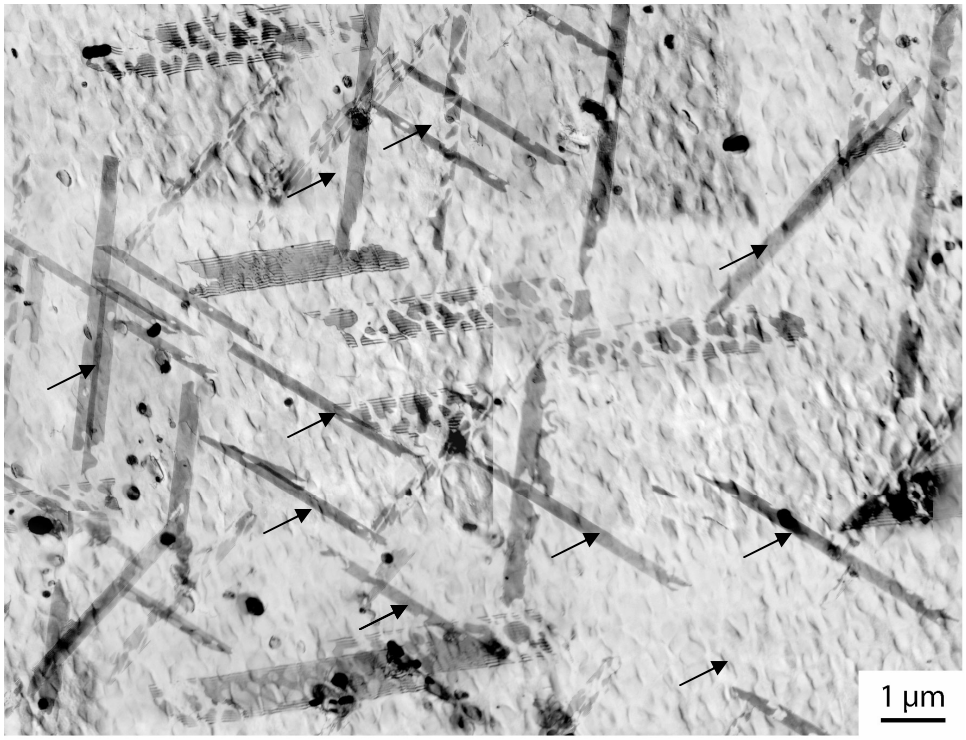

Figure 7

Table 1. Chemical composition in weight percent of the MC2 and NR3 superalloys.

	Ni	Cr	Co	Mo	Al	Ti	W	Ta	Hf	Zr	C	B
MC2	Base	8	5	2	5	1.5	8	6	-	-	-	-
NR3	Base	11.8	14.6	3.3	3.6	5.5	-	-	0.3	0.05	0.02	0.01

Table 2. Statistic values defining the microstructures of the NR3 and MC2 superalloys.

	Medium width of γ' precipitates (nm)	Medium width d of γ channels (nm)
NR3	340 for secondary γ' 35 for tertiary γ'	5 < d < 250 < d > = 52 between tertiary
MC2	400	20 < d < 100 < d > = 50

Captions

Table 1: Chemical compositions (wt. %) of the MC2 and NR3 superalloys.

Table 2: Statistical values defining the microstructures of the NR3 and MC2 superalloys.

Figure 1: Precipitation microstructures: a) polycrystalline NR3 superalloy and b) MC2 single crystal superalloy.

Figure 2: *Post mortem* observations after creep (650 MPa, 700°C, 140 h). Examples of the decorrelated movement of partial dislocations in the NR3 superalloy.

Figure 3: *In situ* dynamic sequence (T = 20°C): three steps in the decorrelated movement of partial dislocations in the NR3 superalloy.

Figure 4: *In situ* dynamic sequence (T = 850°C): three steps in the decorrelated movement of partial dislocations in the MC2 superalloy.

Figure 5: Shearing of γ' particles by the leading partial p_1 after the decorrelation process has taken place. The trailing partial p_2 is stopped.

Figure 6: Line tension calculated in the frame of anisotropic elasticity using DISDI software. The different constants used correspond to the γ-phase at 850°C: C_{11} = 136 GPa, C_{12} = 73 GPa and C_{44} = 89 GPa (Pollock and Argon 1994) and Γ = 20 mJ/m^2 (Benyoucef et al. 1995). A perfect undissociated dislocation (1), a partial belonging to a perfect dissociated dislocation (2) and an isolated partial dislocation (3) are considered as a function of their character ϕ.

Figure 7: Straining microstructure observed in the NR3 alloy creep-strained at 700°C under 650 MPa and until 0.2 % of plastic deformation.